Journal of Nuclear Medicine, published on August 13, 2015 as doi:10.2967/jnumed.115.160770

Discrimination between brown and white adipose tissue using a two-point Dixon water-fat separation method in simultaneous PET/MRI

Original research

Daniela Franz[1], Dimitrios C. Karampinos[1], Ernst J. Rummeny[1], Michael Souvatzoglou[2,3], Ambros J. Beer[2,3], Stephan G. Nekolla[2], Markus Schwaiger[2], Matthias Eiber[2]

[1]Department of Diagnostic and Interventional Radiology, Technische Universität München, Munich, Germany
[2] Department of Nuclear Medicine, Technische Universität München, Munich, Germany
[3] Department of Nuclear Medicine, Universität Ulm, Ulm, Germany

First and corresponding author: Daniela Franz, MD (resident), *daniela.franz@tum.de, Phone: +49 89 4140 2621, Fax: +49 89 4140 4435*

Word count: 4675 (including title page, abstract, text, references, figure legends, tables)

Short running Title: Discriminating BAT/WAT with PET/MRI

Abstract

The purpose of the study was to evaluate signal-fat-fraction (SFF)-analysis based on a 2-point-Dixon water-fat separation method in whole-body simultaneous PET/MRI for identifying brown adipose tissue (BAT) and discriminating it from white adipose tissue (WAT) using cross-validation via PET.

Methods:

This retrospective, internal review board–approved study evaluated 66 PET/MRI-examinations of 33 pediatric patients (mean age 14.7 years; range 7.4-21.4). Eleven elderly patients were evaluated as control (mean age 79.9 years, range 76.3-88.6). Pediatric patients were divided into two groups-with and without metabolically active supraclavicular BAT. Standard of reference for the presence of BAT was at least one PET-examination showing 18F-FDG-uptake. PET/MRI included a 2-point-Dixon water-fat-separation method. Signal intensities in ROIs on fat and water images and mean standardized uptake values (SUV_{mean}) were determined bilaterally in supraclavicular and gluteal fat depots. SFF was calculated from the ratio of fat signal over summed water- and fat signal. Statistical analysis was conducted by using Student´s t-test and correlation analysis.

Results:

SFF was significantly lower ($p<0.0001$) in supraclavicular BAT compared to gluteal WAT in all pediatric subjects. Supraclavicular SFF was significantly higher in the control than in the pediatric group ($p<0.0001$). In PET-positive patients with multiple examinations, SFF stayed stable while SUV_{mean} fluctuated (median intraindividual change 5% vs. 91%). No significant correlation between SUV_{mean} and SFF could be observed for BAT.

Conclusion:

The results demonstrate that MRI-SFF-analysis is a reproducible imaging modality for detection of human BAT and discrimination from WAT. SFF-values of BAT are independent from its metabolic activity, making SFF a more reliable parameter for BAT than the commonly used PET-signal. However, with intent to investigate both the composition of BAT as well as its activation status hybrid PET/MRI might provide supplementary information.

Key Words: Brown adipose tissue; signal-fat-fraction; simultaneous PET/MRI

INTRODUCTION

Brown adipose tissue (BAT) is an organ responsible for thermogenesis through consummation of fat in response to certain stimuli such as low temperatures (*1, 2*). BAT can be mostly found in supraclavicular and cervical depots in humans, while more anatomical sites (e.g., suprarenal, mediastinal) have been described in post-mortem studies (*3*).

On a cellular level, in comparison to white adipose tissue (WAT), BAT is an extensively vascularized tissue characterized by smaller adipocytes than those in WAT, containing a centrally located nucleus, multiple triglyceride droplets and a vast amount of iron-containing mitochondria and intracellular water (*4*). BAT can be found predominantly in babies and children, but several studies published during the last years have demonstrated metabolically active BAT in adults (*5-7*). This corroborates observations of the aforementioned post-mortem study that, even though there is an age relationship with BAT distribution, BAT is still present in adults (*3*). Notably, there is evidence that adults exhibit two types of BAT, having the same cell morphology but originating from different progenitors (*8*).

Prevalence of obesity and its comorbidities is growing worldwide, leading to a global health issue and socioeconomic problem (*9*). Different studies have investigated BAT recruitment as a therapeutic approach for obesity, elevated triglyceride concentrations and type 2 diabetes in rodents (*10-13*). Furthermore, studies in adults, pediatrics and adolescents showed an inverse correlation between obesity and the presence of metabolically active BAT determined by 18F-FDG PET/CT examinations (*6, 14, 15*), rendering BAT an increasingly relevant role in the fight against obesity in humans (*16-18*). The development of precise and reliable tools for the quantification of body fat, its

distribution and determination of its type are highly needed. Several recent studies have investigated 18F-FDG PET for identification of BAT making PET/CT a reference modality in BAT imaging (*7, 14, 19, 20*) in particular as it is depicting metabolic activity of BAT depots. Nevertheless, magnetic resonance imaging (MRI) is currently thought of as the best tool in the evaluation of body fat due to its detailed soft tissue characterization, superior spatial resolution and the lack of exposing the patient to ionizing radiation (*21, 22*). Therefore, MRI could represent an encouraging alternative to PET/CT to study BAT independently from its metabolic activity, especially in healthy populations.

Common parameters for the detection of BAT by MRI are the signal-fat-fraction (SFF) and the proton-density fat-fraction (PDFF), defined as the ratio of fat signal intensity over the sum of water and fat signal intensities. SFF and PDFF values reflect the different water content in BAT and WAT and have been approved in several studies (*23-25*). Some studies tried to relate the results of separate 18F-FDG PET/CT and MRI examinations in a small number of patients proven to have metabolically active BAT on earlier 18F-FDG PET/CT (*26, 27*), evaluating metabolic activity and signal characteristics on MRI successively. Simultaneous 18F-FDG PET/MRI represents a method to assess metabolic activity and MRI-signal in a single examination without allowing interference e.g. by external factors such as cold exposition in between scans.

The present study is based on the hypothesis 1) that MRI-SFF-analysis is a reproducible imaging modality for detection of human BAT and discrimination from WAT and 2) that the presence of BAT is independent from BAT being metabolically active. A retrospective analysis using data from whole-body simultaneous 18-F-FDG PET/MRI studies in pediatric subjects based on a 2-point-Dixon water-fat separation method was

pursued for identifying BAT with MRI and discriminating it from WAT using cross-validation via PET, choosing elderly subjects as a control group.

MATERIALS AND METHODS

Subjects

In a retrospective study, all pediatric subjects (age ≤ 21 years at time of examination) who underwent 18F-FDG PET/MRI due to oncological diagnoses between September 2011 and April 2014 were retrieved from the institutional database. Institutional review board approved was obtained and all subjects and/or their legal guardians gave informed assent/consent. Exclusion criteria were standard contraindications for MRI examinations.

A total of 66 18F-FDG PET/MRI examinations in 33 subjects were evaluated. Mean age of the pediatric subjects examined was 14.7 years (range 7.4-21.4). The group of pediatric subjects was composed of 9 female individuals (mean age 16.3 years; range 9.5-21.4) and 24 male individuals (mean age 14.1 years, range 7.4-19.2 years) (Figure 1). As control group, 18F-FDG PET/MRI data from 11 elderly subjects (7 male, 4 female; mean age 79.9 years, range 76.3-88.6) were evaluated. Exclusion criteria again were standard contraindications for MRI examinations. The mean injected activity of 18F-FDG was 254 MBq (SD 97, range 75-471). Subjects fasted 6h before tracer injection, and blood glucose levels were measured just before injection, with a cut-off of 150 mg/dL. Sedation, which could potentially influence BAT activity (*28*) was not used in any patients.

Whole-body simultaneous 18F-FDG PET/MRI

All examinations were performed on a fully integrated whole-body hybrid system (Biograph mMR; Siemens Healthcare, Erlangen, Germany). 18F-FDG PET/MRI was acquired at a mean of 105 min after tracer injection (range 63-175).

For all 18F-FDG PET/MRI examinations, the following protocol was used. First, MRI localizer sequences were acquired to determine the location and number of PET bed positions. Secondly, the PET emission scans were initiated, with an emission time of 4 min per bed position. A 2-point T1-weighted coronal 3-dimensional Dixon spoiled gradient-echo sequence (VIBE Dixon sequence) combined with a water-fat separation method was acquired for attenuation correction purposes simultaneously at the beginning of every PET measurement. To minimize motion artifacts from incomplete breath-holds, a centric k-space acquisition was used. Imaging parameters and setup for the spoiled gradient-echo sequence are summarized in Table 1. A water-fat separation was performed based on the raw images yielding four different image series: a) in-phase, b) opposed-phase, c) water-weighted and d) fat-weighted. Depending on their oncological diagnosis further MRI-sequences including at least a coronal T1 weighted TSE sequence in all patients were acquired. All images were uploaded to a dedicated workstation (Syngo MMWP, Siemens Healthcare).

Image Analysis

Image datasets were analyzed by 2 experienced readers in consensus (2 years and 8 years) who were blinded to the patients´ history.

In order to identify regions of BAT, the supraclavicular/cervical region was examined, since areas of adipose tissue can be easily identified and delineated in this area on

anatomical images and BAT in this region has been broadly characterized in PET/CT and autopsy studies (*2, 3, 7, 20*). For areas of WAT, gluteal fat depots were evaluated since they are definable in every patient and it is expected to find exclusively WAT in this region (*3, 29*).

For every dataset with 18F-FDG-avid supraclavicular fat depots, regions of interest (ROIs) were placed in the PET-dataset bilaterally into the supraclavicular fat depots, automatically delineating the shape of the 18F-FDG-avid fat depots (50% isocontour). If no or only low 18F-FDG-uptake could be detected, ROIs were placed into the fat-weighted MR-image, automatically delineating the region with high signal on fat-weighted images- i.e. the fat depot itself. For measurement of WAT, round ROIs were placed into gluteal subcutaneous fat depots bilaterally on the fat-weighted image.

The ROIs were automatically transferred to the co-registered images (fat-weighted and water-weighted images/water-weighted and PET-images respectively). Mean signal intensities on fat- and water-weighted images as well as mean SUV_{mean} of the PET-dataset were noted. Signal-fat-fraction (SFF) for BAT and WAT was calculated using the following formula: $\frac{\text{fat signal intensity}}{(\text{fat signal intensity} + \text{water signal intensity})}$.

Finally, subjects were divided into two groups: the PET-positive group with moderate to high 18F-FDG-uptake ($SUV_{mean}>1$) in at least one 18F-FDG PET examination and the PET-negative group with no or low uptake in all available examinations.

Statistical Analysis

Data are expressed as mean (SD, range) if not otherwise denoted. An unpaired Student´s t-test was used to compare the SFF and SUV_{mean} in supraclavicular/cervical

and gluteal adipose tissue as well as to compare the SFF of the study group and the control group. Linear regression analysis was used to determine the correlation coefficient between SFF and SUV_{mean}. In all experiments a probability value of less than 0.05 was considered significant. Statistical analysis was performed using MedCalc statistical software (MedCalc Software Version 7.2.0.2, Ostend, Belgium).

RESULTS

First, the numbers of PET-positive and PET-negative subjects were determined. Of the 33 examined pediatric subjects, 16 were found to have 18F-FDG-avid, metabolically active supraclavicular/cervical fat depots in at least one of their examinations suggestive of brown adipose tissue. Therefore these subjects were determined as PET-positive. Of those 16 subjects, 12 had multiple examinations, resulting in a total number of 38 examinations. In all other pediatric subjects (n=17, total number of 28 examinations) and the 11 subjects in the control group, no metabolically active adipose tissue was found (Figure 1). Thus, these subjects were determined as PET-negative.

Within the group of PET-positive pediatric subjects, MRI-based mean SFF was 0.70 in supraclavicular BAT (SD 0.08, range 0.5-0.88) and 0.92 in gluteal WAT (SD 0.04, range 0.84-0.97). This resulted in a highly significant difference between the two types of fat ($p<0.0001$) (Table 2).

In the 12 PET-positive subjects with multiple examinations, intraindividual SFF in supraclavicular fat depots was relatively constant at all measurements with a median percentage change of 5% (range 0-39%). In contrast, intraindividual changes in 18F-

FDG uptake were considerably higher with a median difference of 91% for the SUV_{mean} (range 10-5621%). In gluteal depots median change in SFF was 2% (range 0-9%) while median change in SUV_{mean} was 39% (range 0-117%). SFF and SUV_{mean} in supraclavicular and gluteal fat depots of all examinations in the PET-positive subjects are shown in Figure 2. Due to this relatively stable SFF and highly variable SUV_{mean} no correlation between SFF in supraclavicular fat depots and SUV_{mean} could be found ($r = -0.125$; $p=0.304$).

Within the group of PET-negative pediatric subjects, MR-based mean SFF was 0.76 in supraclavicular depots (SD 0.1, range 0.32-0.94) and 0.91 in gluteal fat tissue (SD 0.04, range 0.81-0.97). This also resulted in a highly significant difference ($p<0.0001$) (Table 2).

With regard to all pediatric patients (PET-positive and PET-negative subjects), SFF still differed significantly in supraclavicular fat depots compared to gluteal fat depots: mean supraclavicular SFF was 0.73 (SD 0.1, range 0.32-0.94) and mean gluteal SFF was 0.91 (SD 0.04, range 0.81-0.97), resulting in a p-value of <0.0001.

In the control group (n=11), mean SFF in supraclavicular fat depots was 0.90 (SD 0.02, range 0.84-0.94). Mean SFF in gluteal depots was 0.93 (SD 0.03, range 0.86-0.97). SFF in supraclavicular fat thus differed between pediatric subjects and the control group ($p<0.0001$). No significant difference of the SFF in gluteal adipose tissue could be observed between pediatric and control subjects ($p=0.13$). Remarkably, the range of the supraclavicular SFF in the control group was comparable to that of gluteal fat depots in the pediatric group (Figure 3).

DISCUSSION

The results of the study indicate that 1) SFF determined by the 2-point VIBE Dixon sequence is lower in BAT compared to WAT in children and 2) SFF is independent from the metabolic activity of the tissue as determined by 18F-FDG PET. Thus SFF represents a robust parameter for the identification of BAT, suggesting that BAT can be identified by using MRI only.

The results of the present study suggest that using a 2-point Dixon water-fat separation method, mean SFF in pediatric subjects is significantly lower in supraclavicular/cervical (brown) fat depots compared to gluteal subcutaneous (white) fat depots. This finding confirms that MRI using the described Dixon-method is able to distinguish between these types of adipose tissue based on the higher water content of BAT (*24, 30*) using a relatively fast 2-point Dixon water-fat separation method acquired for attenuation correction in simultaneous 18F-FDG PET/MRI.

The advantage of using simultaneous 18F-FDG PET/MRI in our study lies in the fact that the presence of BAT can be proven by showing metabolically active adipose tissue in 18F-FDG PET and by evaluating the corresponding SFF at the same time. This allowed an initial cross-validation of MRI with respect to its further use to distinguish between different types of adipose tissue (*24, 31*). Consequently differences in SFF between gluteal and cervical adipose tissue in patients with metabolically active cervical fat can be attributed to the presence of different types of adipose tissue, i.e. brown and white adipose tissue.

Furthermore, with cervical and gluteal SFF values in PET-negative patients comparable to those in PET-positive patients and by prior validating the use of SFF in PET-positive subjects to detect BAT, it can be concluded that in PET-negative patients BAT was also present in the cervical region, only not being metabolically active by the time of the examination. Consequently, BAT can possibly be detected by sole determination of the SFF via the 2-point Dixon water-fat separation method used in this study, even in patients without a positive PET-signal.

In the control group composed of elderly subjects (≥76 years), supraclavicular SFF values were substantially higher than in the pediatric group, with ranges comparable to that in gluteal fat depots in both pediatric and elderly subjects (Figure 3). Histologically, BAT was never shown to be present in gluteal fat (*3, 29*), so it can be hypothesized that both the pediatric and control group had WAT in gluteal fat depots. Consequently, the supraclavicular SFF range in the control group also points to WAT.

The reason for the statistical significant difference between supraclavicular and gluteal SFF in the control group is not completely clear. With regard to the range of supraclavicular and gluteal SFF in this population (Figure 3) a broad overlap is present. It could be hypothesized that a minimal amount of BAT is still present in the supraclavicular region of elderly people leading to a small but statistical significant drop of SSF. However, no histomorphological data are available at the present.

With regard to the longitudinal analysis of SFF compared to 18F-FDG PET, another crucial result of this study was that metabolic activity as determined by PET-based SUV-analysis showed no correlation with SFF in subjects with metabolically active BAT. So

far, it was not clear whether BAT is subject to short-term changes in metabolic activity ("sleeping" BAT) depending on factors like nutritional status and environmental conditions (e.g., cold stimulation), or whether the human adipose organ is "plastic", comparable to that of rodents where adipocytes in BAT and WAT populations can reversibly turn into one another as short-term reaction to stimuli such as cold exposure (*4, 32, 33*).

Using 18F-FDG PET/CT the detection of BAT is limited to the evidence of metabolic activity by a positive 18F-FDG-uptake in PET with no further tissue characterization being possible. Thus, for tissue characterization in longitudinal studies with PET/CT, histology samples would be required, ideally sampled shortly after the PET/CT examination to avoid distortion by possible short-term plasticity of the adipose organ.

By using PET/MRI in the present study, it was possible to perform simultaneous measurements of metabolic activity as determined by SUV_{mean} and of accurately co-localized tissue composition as determined by SFF not being influenced by a potential change in the metabolic status and composition of BAT using sequential examinations. In subjects with multiple examinations, intraindividual SUV_{mean} fluctuated massively with a median change of 91% while intraindividual SFF was subject to only minor variations with a median change of 5% (Figure 2).This indicates that the composition of the adipose tissue as determined by calculation of SFF stays relatively stable independent from the current metabolic activity (see example: Figure 4). Consequently our data argue against the hypothesis of BAT being a "plastic" tissue and is in favor of its constant existence with only a different grade of metabolic activity. However the hypothesis has to be proven in further studies. Hereby, the present data suggest that

BAT being not detectable on PET-images due to its metabolic inactivity can potentially be identified using SFF-analysis.

The present study has some limitations. First, BAT can occur in mixed clusters with white adipocytes in humans (*4, 33*), thus a certain SFF range is only suggestive of the presence of BAT as it is an average value of the SFF within one fat depot. Furthermore, partial volume effects have to be considered, especially when low resolution PET data are used for setting the ROI, as SFF cannot differentiate between intracellular water content and non-lipid tissue portions (e.g. from vessels) within a voxel.

Second, SFF is not as accurate as the so called proton density fat fraction (PDFF). SFF refers to MR signal attributable to fat and is confounded by various MRI related properties such as T1 or T2*, thus values can differ when changing acquisition parameters, while PDFF refers to the fraction of mobile protons attributable to fat and removes biases such as T1 and T2*, and is potentially more accurate since it uses multi-peak fat spectral fitting (*25*). Water-fat separation methods applied on six-echo gradient echo data can extract PDFF and are thereby free of any confounding effects (*31*). Nevertheless, SFF based on a water-fat separation methods applied on two-echo gradient echo data is a promising tool to verify the presence of BAT without radiation exposure as in PET. Thus compared to PET, SFF and PDFF are more suited as a screening method for detecting BAT or as a method for longitudinal of fat distribution.

Third, the present study was limited by the predominantly male study population (n=24) which was not intentional. Previous PET/CT studies provide conflicting information about gender dependence of BAT in pediatric cohorts (*15, 20*) and further investigations should also determine gender effects on presence and development of BAT.

Fourth, histology was not used as gold standard diagnostic reference in differentiating WAT from BAT due to ethical and practical reasons. However, 18-FDG-uptake is evidently related to metabolically active BAT (*5, 34*). Furthermore, supraclavicular SFF in PET-positive and PET-negative pediatric patients were comparable and in both groups significantly different from gluteal subcutaneous WAT, which in turn was comparable to the supraclavicular and gluteal fat in the control subjects. Considering this together with results from autopsy studies (*3*) it can be assumed that BAT is present within the supraclavicular/cervical adipose tissue in pediatric subjects and the different adipose tissue in pediatric subjects (gluteal) and elderly subjects (supraclavicular and gluteal) is WAT.

CONCLUSION

18F-FDG PET/MRI is a promising tool for combined morphological and functional evaluation of BAT especially using it for cross validating of a MR-technique for discrimination between WAT and BAT. The present preliminary data show that a 2-point Dixon sequence acquired for attenuation correction in 18F-FDG PET/MRI can be used for reliable SFF-analysis. Hereby, SFF represents a robust method for the differentiation of BAT and WAT being independent from the metabolic activation of BAT. The methods used in this study can potentially be applied in studies on human BAT in healthy cohorts and in longitudinal studies for monitoring BAT characteristics in response to stimulation and therapeutic interventions. Thus further studies are promising and warranting, especially focusing on determining a reliable threshold between BAT and WAT for visualizing and evaluating BAT mass semi-quantitatively. In addition, when information

concerning the composition and extent of BAT and its specific activation status are needed the use of MRI and PET by hybrid PET/MRI might provide supplementary information.

Financial Disclosures: The authors have nothing to disclose.

References:

1. Shabalina IG, Kramarova TV, Nedergaard J, Cannon B. Carboxyatractyloside effects on brown-fat mitochondria imply that the adenine nucleotide translocator isoforms ANT1 and ANT2 may be responsible for basal and fatty-acid-induced uncoupling respectively. *Biochem J.* 2006;399:405-414.

2. Enerback S. Human brown adipose tissue. *Cell Metab.* 2010;11:248-252.

3. Heaton JM. The distribution of brown adipose tissue in the human. *J Anat.* 1972;112:35-39.

4. Frontini A, Cinti S. Distribution and development of brown adipocytes in the murine and human adipose organ. *Cell Metab.* 2010;11:253-256.

5. Cypess AM, Lehman S, Williams G, et al. Identification and importance of brown adipose tissue in adult humans. *N Engl J Med.* 2009;360:1509-1517.

6. van Marken Lichtenbelt WD, Vanhommerig JW, Smulders NM, et al. Cold-activated brown adipose tissue in healthy men. *N Engl J Med.* 2009;360:1500-1508.

7. Virtanen KA, Lidell ME, Orava J, et al. Functional brown adipose tissue in healthy adults. *N Engl J Med.* 2009;360:1518-1525.

8. Betz MJ, Enerback S. Human Brown Adipose Tissue: What We Have Learned So Far. *Diabetes.* 2015;64:2352-2360.

9. Ogden CL, Carroll MD, Kit BK, Flegal KM. Prevalence of obesity and trends in body mass index among US children and adolescents, 1999-2010. *JAMA.* 2012;307:483-490.

10. Ghorbani M, Himms-Hagen J. Appearance of brown adipocytes in white adipose tissue during CL 316,243-induced reversal of obesity and diabetes in Zucker fa/fa rats. *Int J Obes Relat Metab Disord.* 1997;21:465-475.

11. Kim H, Pennisi PA, Gavrilova O, et al. Effect of adipocyte beta3-adrenergic receptor activation on the type 2 diabetic MKR mice. *Am J Physiol Endocrinol Metab.* 2006;290:E1227-1236.

12. Himms-Hagen J, Cui J, Danforth E, Jr., et al. Effect of CL-316,243, a thermogenic beta 3-agonist, on energy balance and brown and white adipose tissues in rats. *Am J Physiol.* 1994;266:R1371-1382.

13. Bartelt A, Bruns OT, Reimer R, et al. Brown adipose tissue activity controls triglyceride clearance. *Nat Med.* 2011;17:200-205.

14. Vijgen GH, Bouvy ND, Teule GJ, Brans B, Schrauwen P, van Marken Lichtenbelt WD. Brown adipose tissue in morbidly obese subjects. *PLoS One.* 2011;6:e17247.

15. Drubach LA, Palmer EL, 3rd, Connolly LP, Baker A, Zurakowski D, Cypess AM. Pediatric brown adipose tissue: detection, epidemiology, and differences from adults. *J Pediatr.* 2011;159:939-944.

16. Boss O, Farmer SR. Recruitment of brown adipose tissue as a therapy for obesity-associated diseases. *Front Endocrinol (Lausanne).* 2012;3:14.

17. Nedergaard J, Bengtsson T, Cannon B. New powers of brown fat: fighting the metabolic syndrome. *Cell Metab.* 2011;13:238-240.

18. Bartelt A, Merkel M, Heeren J. A new, powerful player in lipoprotein metabolism: brown adipose tissue. *J Mol Med (Berl).* 2012;90:887-893.

19. Yoneshiro T, Aita S, Matsushita M, et al. Brown adipose tissue, whole-body energy expenditure, and thermogenesis in healthy adult men. *Obesity (Silver Spring).* 2011;19:13-16.

20. Gilsanz V, Smith ML, Goodarzian F, Kim M, Wren TA, Hu HH. Changes in brown adipose tissue in boys and girls during childhood and puberty. *J Pediatr.* 2012;160:604-609 e601.

21. Hu HH, Kan HE. Quantitative proton MR techniques for measuring fat. *NMR Biomed.* 2013;26:1609-1629.

22. van der Meer RW, Lamb HJ, Smit JW, de Roos A. MR imaging evaluation of cardiovascular risk in metabolic syndrome. *Radiology.* 2012;264:21-37.

23. Lunati E, Marzola P, Nicolato E, Fedrigo M, Villa M, Sbarbati A. In vivo quantitative lipidic map of brown adipose tissue by chemical shift imaging at 4.7 Tesla. *J Lipid Res.* 1999;40:1395-1400.

24. Hu HH, Perkins TG, Chia JM, Gilsanz V. Characterization of human brown adipose tissue by chemical-shift water-fat MRI. *AJR Am J Roentgenol.* 2013;200:177-183.

25. Reeder SB, Cruite I, Hamilton G, Sirlin CB. Quantitative Assessment of Liver Fat with Magnetic Resonance Imaging and Spectroscopy. *J Magn Reson Imaging.* 2011;34:spcone.

26. Chen YC, Cypess AM, Chen YC, et al. Measurement of human brown adipose tissue volume and activity using anatomic MR imaging and functional MR imaging. *J Nucl Med.* 2013;54:1584-1587.

27. Reddy NL, Jones TA, Wayte SC, et al. Identification of brown adipose tissue using MR imaging in a human adult with histological and immunohistochemical confirmation. *J Clin Endocrinol Metab.* 2014;99:E117-121.

28. Dicker A, Ohlson KB, Johnson L, Cannon B, Lindahl SG, Nedergaard J. Halothane selectively inhibits nonshivering thermogenesis. Possible implications for thermoregulation during anesthesia of infants. *Anesthesiology.* 1995;82:491-501.

29. Sacks H, Symonds ME. Anatomical locations of human brown adipose tissue: functional relevance and implications in obesity and type 2 diabetes. *Diabetes.* 2013;62:1783-1790.

30. Hu HH, Yin L, Aggabao PC, Perkins TG, Chia JM, Gilsanz V. Comparison of brown and white adipose tissues in infants and children with chemical-shift-encoded water-fat MRI. *J Magn Reson Imaging.* 2013;38:885-896.

31. Hu HH, Wu TW, Yin L, et al. MRI detection of brown adipose tissue with low fat content in newborns with hypothermia. *Magn Reson Imaging.* 2014;32:107-117.

32. Himms-Hagen J, Melnyk A, Zingaretti MC, Ceresi E, Barbatelli G, Cinti S. Multilocular fat cells in WAT of CL-316243-treated rats derive directly from white adipocytes. *Am J Physiol Cell Physiol.* 2000;279:C670-681.

33. Cinti S. Transdifferentiation properties of adipocytes in the adipose organ. *Am J Physiol Endocrinol Metab.* 2009;297:E977-986.

34. Hu HH, Tovar JP, Pavlova Z, Smith ML, Gilsanz V. Unequivocal identification of brown adipose tissue in a human infant. *J Magn Reson Imaging.* 2012;35:938-942.

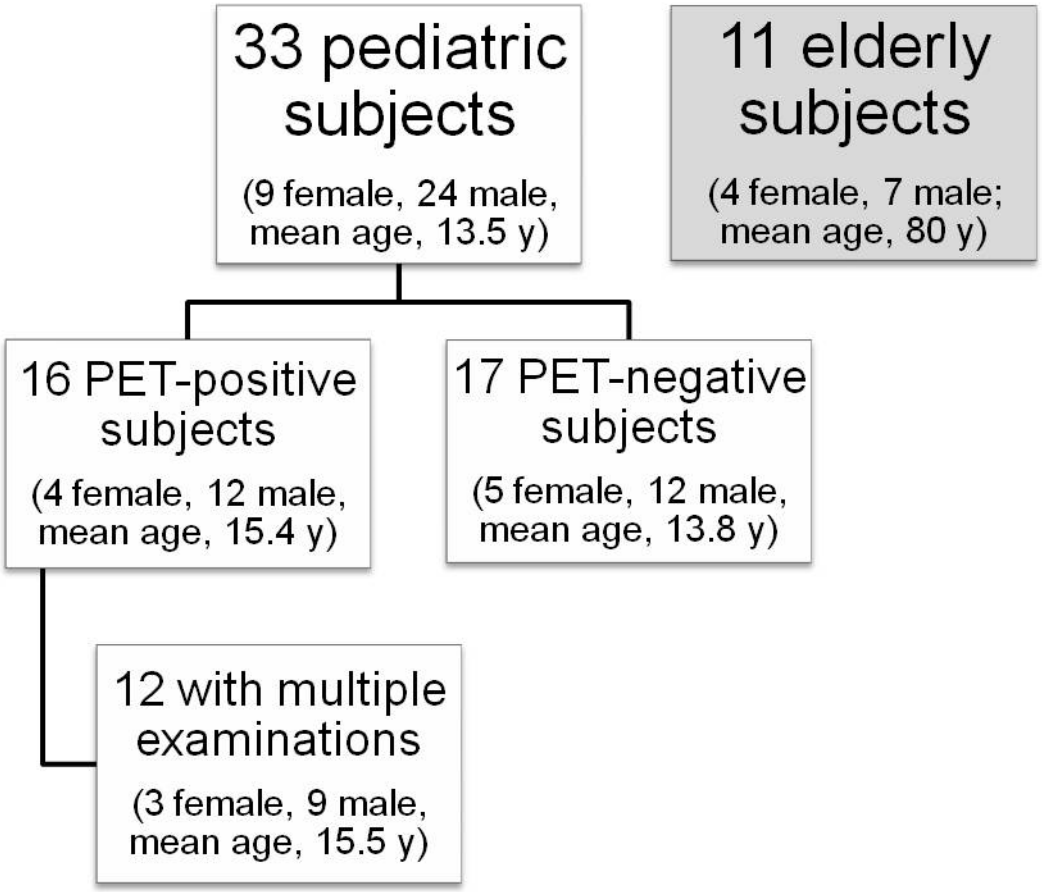

FIGURE 1- Age and gender of the study and control cohort (mean age at time of examination)

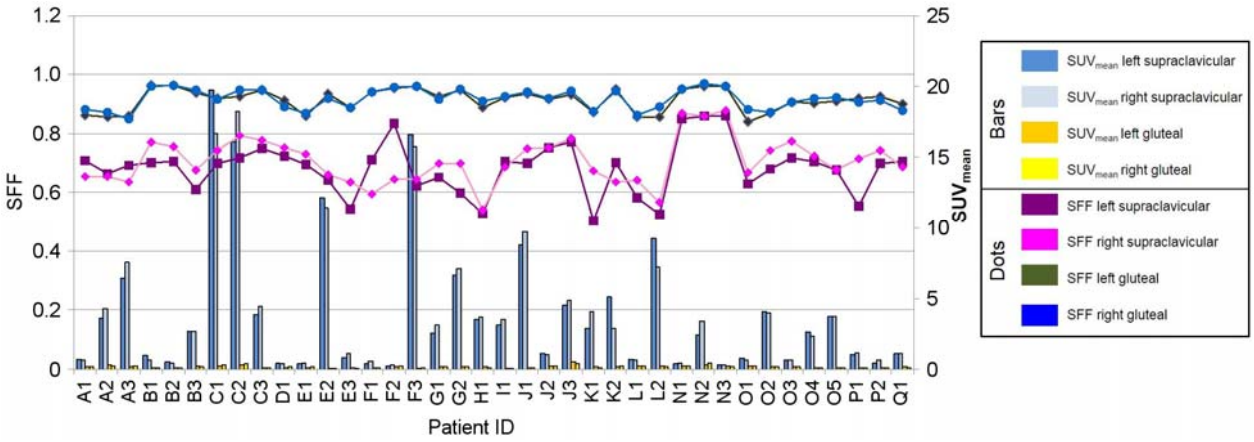

FIGURE 2 - SFF and SUV_{mean} in supraclavicular and gluteal fat depots in PET-positive subjects. Each patient is represented by a specific letter. In patients with multiple examinations the number displays the individual examination.

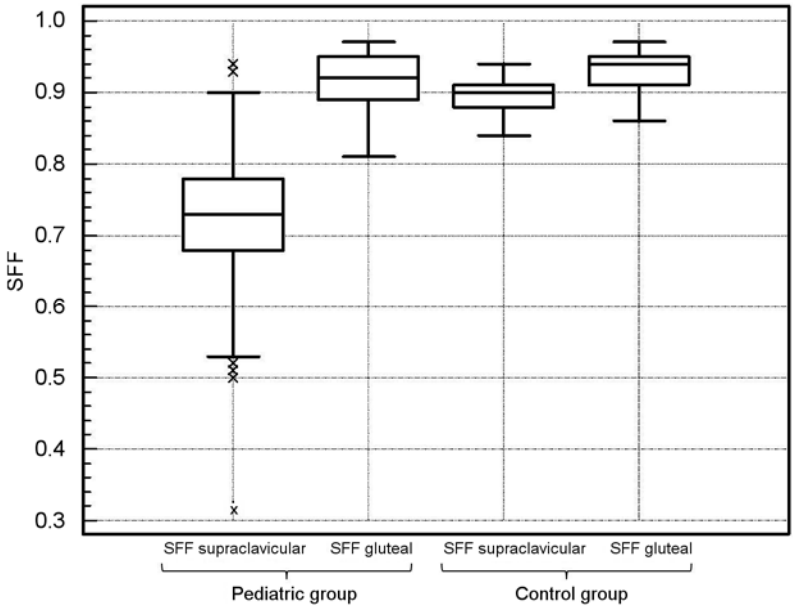

FIGURE 3 - SFF in supraclavicular and gluteal fat depots in pediatric group compared to control group

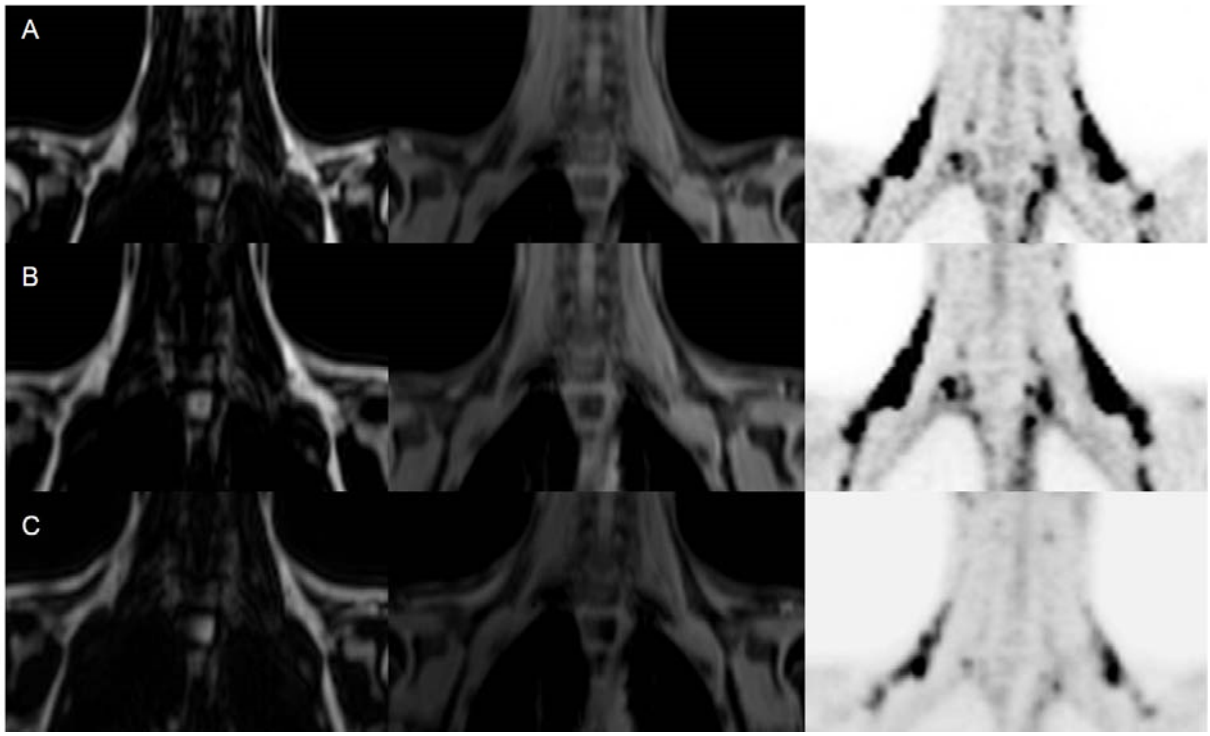

FIGURE 4 - Image examples – Patient C at three consecutive examinations (A-C). Left=fat-weighted MR-image, middle=water-weighted MR-image, right=PET-image. Black spots on PET-image indicating metabolically active BAT. Note the varying strength in PET-signal (SFF at examination A: left/right 0.70/0.74; B: 0.72/0.79; C: 0.75/0.78. SUV_{mean} at examination A: left/right 19.75/16.66; B: 16.09/18.25; C: 3.86/4.46)

TABLE 1- Technical Parameters of MR Sequence Used in Study

Sequence	T1-weighted VIBE Dixon
TR/TE (ms)	3.60/1.23–2.46*
Slice thickness (mm)	3.12
Gap (%)	0
Matrix	192 × 121
In-plane resolution (mm)	4.1 × 2.6
Field of view (mm)	500
% phase field of view	100
Acquisition time (min:s)	0:19
Number of excitations	1
iPAT factor	2

- * Fat-saturation techniques with Dixon require 2 repetition times.

- TR/TE = repetition time/echo time; iPAT = integrated parallel acquisition technique.

TABLE 2- Overview of SFF and SUV_{mean} values of PET-positive, PET-negative and control group and p-values

		Supraclavicular mean (SD, range)	**Gluteal** mean (SD, range)	**p-value**
SFF	**PET-positive** n=16	0.70 (0.08, 0.50-0.88)	0.92 (0.04, 0.84-0.97)	<0.0001
	PET-negative n=17	0.76 (0.1, 0.32-0.94)	0.91 (0.04, 0.81-0.97)	<0.0001
	Control n=11	0.90 (0.02, 0.84-0.94)	0.93 (0.03, 0.86-0.97)	0.0026
SUV_{mean}	**PET-positive** n=16	4.0 (4.77, 0.29-19.75)	0.20 (0.09, 0.08-0.50)	<0.0001
	PET-negative n=17	0.45 (0.17, 0.24-0.91)	0.20 (0.09, 0.02-0.44)	<0.0001
	Control n=11	0.52 (0.11, 0.32-0.68)	0.23 (0.07, 0.14-0.35)	<0.0001